WORLD OF HEALTH 2021; (4) 64-69

URINARY BLADDER CANCER DIAGNOSIS USING CUSTOMIZED VGG-16 ARCHITECTURES

DIJAGNOSTIKA KARCINOMA MOKRAĆNOG MJEHURA PRIMJENOM PRILAGOĐENIH VGG-16 ARHITEKTURA

Ivan Lorencin[1]*, Sandi Baressi Šegota[1], Nikola Anđelić[1], Vedran Mrzljak[1], Klara Smolić[2], Josip Španjol[2,3] and Zlatan Car[1]

1 University of Rijeka, Faculty of Engineering, Vukovarska 58, 51000 Rijeka, Croatia
2 Clinical Hosipital Centre Rijeka, Krešimirova ul. 42, 51000, Rijeka
3 University of Rijeka, Faculty of Medicine, Braće Branchetta 20/1, 51000, Rijeka

**Autor za korespodenciju:*
Ivan Lorencin
ilorencin@riteh.hr
University of Rijeka Faculty of Engineering, Department of automation and electronics,
Vukovarska 58, 51000 Rijeka, Croatia

ABSTRACT

Bladder cancer is one of the most common malignancies in men in Croatia. It is characterized by a high recurrence rate and high metastatic potential. For this reason, accurate and timely diagnosis is needed in order to treat bladder cancer as successfully as possible. Cystoscopy as a diagnostic method shows poorer accuracy of Carcinoma in situ (CIS) diagnosis, where every fourth CIS remains undiagnosed. For this reason, the artificial intelligence-based approach is proposed. The standard approach to image classification is utilization of convolutional neural networks (CNN). Literature overview shows a possibility of using pre-defined CNN models, such as VGG-16. VGG-16, in this case, needs to be customized in order to adapt it to four-class classification problem. By using a customized VGG-16 model, high classification performances are achieved. When AdaGrad and AdaMax solvers are used, AUC_{micro} values up to 0.98 are achieved.

SAŽETAK

Karcinom mokraćnog mjehura jedna je od najčešćih zloćudnih bolesti muškaraca u Hrvatskoj. Karakterizira ga visoka stopa recidiva i visok metastatski potencijal. Iz tog je razloga potrebna točna i pravovremena dijagnoza kako bi se što uspješnije liječio. Cistoskopija kao dijagnostička metoda pokazuje lošiju točnost dijagnoze karcinoma in situ (CIS), gdje svaki četvrti CIS ostaje nedijagnosticiran. Iz tog razloga predlaže se pristup zasnovan na umjetnoj inteligenciji. Standardni pristup klasifikaciji slika je upotreba konvolucijskih neuronskih mreža (CNN). Pregled literature upućuje na mogućnost korištenja unaprijed definiranih CNN modela, poput VGG-16. VGG-16, u ovom slučaju, treba prilagoditi kako bi se prilagodio četveroklasnom klasifikacijskom problemu. Korištenjem prilagođenog modela postižu se visoke klasifikacijske performanse. Kada se koriste optimizatori AdaGrad i AdaMax, postižu se vrijednosti AUC_{micro} do 0.98.

INTRODUCTION

Urinary bladder cancer is one of the most common malignancies in the urinary tract, and it represents the fourth most frequent cancer in Croatia (1). The incidence of bladder cancer is 3-4 times higher in the male population. That fact makes it predominantly a male disease. Bladder cancer originates in the uncontrolled growth of mucosal cells with a pronounced tendency to spread to other organs.

There are a number of types of bladder cancer, the most common of which are:

- urothelial carcinoma (2, 3),
- squamous cell carcinoma (4, 5),
- adenocarcinoma (6, 7),
- small cell carcinoma (8, 9) and
- sarcoma (10, 11).

Of the above-mentioned,, urothelial carcinoma is the most common. Other types of urinary bladder cancer are characterized as: rare, very rare and extremely rare. Urothelial carcinoma, that is also called transitional cell carcinoma (TCC), originates in urothelial cells. These cells are located at the inner surface of the urinary bladder. A dominant number of TCCs can be found in form of a papillary, exophytic lesion with low-grade malignancy potential (12).

A limiting circumstance in the diagnosis and treatment of bladder cancer is its marked propensity for recurrence (61% in the first year, 78% in five years) (13). Such a characteristic, together with metastatic potential, is particularly emphasized in the case of High-grade bladder cancers and carcinomas in-situ (CIS). CIS form of the bladder cancer is often manifested as erythematosus flat lesions of the urinary bladder mucosa. For these reasons, it is crucial to determine the correct form of the urinary bladder cancer during diagnostic procedure.

As an endoscopic method, white light cystoscopy has a central role in diagnosis and follow-up. It is characterized by its capability for accurate detection of papillary lesions. On the other hand, detection of flat lesions is difficult, and the possibility of their differentiation in relation to non-malignant, inflammatory changes is reduced.
By reducing the aforementioned claims to numbers, it can be seen that the percentage of correctly diagnosed CIS is only 75%. In other words, one in four CIS remains un-

diagnosed. With the aim of preventing advancement of the disease (14, 15), artificial intelligence (AI) algorithms such as artificial neural network (ANN) could be introduced in order to increase diagnosis accuracy of urinary bladder cancer type (16). Such a need is particularly emphasized in the case of CIS.

Nowadays, AI algorithms have found their place in various branches of science and technology. Their application ranges from marine propulsion systems (17, 18), through energy (19) and satellite surveillance (20) to medicine (21, 22). AI is also being used to combat the current COVID-19 pandemic by modelling the spread of the virus (23, 24).

Alongside above-mentioned applications, AI has found its place in urinary bladder cancer diagnosis. Research presented in (25) proposes an application of convolutional neural network (CNN) in order to classify images obtained with cystoscopy. Data set that consists of 2102 images was divided into two classes (healthy tissue and tumour lesions). Similar approach that resulted with accuracy of 98 % was proposed in (26). Trained CNN model has achieved AUC value of 0.98. The similar approach was proposed in (27), where authors have used pre-defined CNN models trained with a dataset that consists of 18681 images. With this approach, F1 score of 99.52% was achieved. The authors of the research presented in (28) have proposed utilization of edge detector-based hybrid ANN model that follows the CNN methodology. Such an approach resulted with AUC value of 0.99.

From literature overview, it can be seen that CNN is widely used AI technique for urinary bladder cancer diagnosis. For these reasons, the aim of this research was to utilize VGG-16, a CNN-based architecture, in order to differentiate types of urinary bladder cancer in order to increase accuracy of CIS diagnosis. Such differentiation was performed in four classes: high-grade carcinoma, low-grade carcinoma, CIS and non-cancer tissue.

METHODS AND MATERIALS

In the following section, a brief description of used dataset used during this research is provided. Alongside dataset description, a description of VGG-16 convolutional neural network architecture is given.

Table 1: Overview of VGG-16 architecture

Layer	Type	Feature map	Size	Kernel size	Activation function
Input	Image	1	224 X 224 X 1	-	-
1	2 X C	96	224 X 224 X 64	3 X 3	ReLU
	P	64	112 X 112 X 64	3 X 3	-
3	2 X C	128	112 X 112 X 128	3 X 3	ReLU
	P	256	56 X 56 X 128	3 X 3	-
5	2 X C	256	56 X 56 X 256	3 X 3	ReLU
	P	384	28 X 28 X 256	3 X 3	
7	3 X C	512	28 X 28 X 512	3 X 3	ReLU
	P	256	14 X 14 X 512	3 X 3	
10	3 X C	512	14 X 14 X 512	3 X 3	ReLU
	P	512	7 X 7 X 512	3 X 3	-
13	FC	-	25088	-	ReLU
14	FC	-	4096	-	ReLU
15	FC	-	4096	-	ReLU
Output	FC	-	4	-	Softmax

DATA SET DESCRIPTION

The procedure for urinary bladder cancer diagnosis using VGG-16 was based on utilization of a high performance computing (HPC) workstation in order to classify images of urinary bladder mucosa. Images were obtained with a cystoscope and uploaded to HPC workstation, where trained VGG-16 model is implemented. According to VGG-16 output, the medical finding was determined. Such a process is presented with dataflow diagram shown in Figure 1.

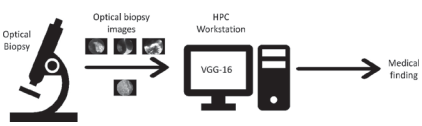

Figure 1: Dataflow diagram of VGG-16 utilization for urinary bladder cancer diagnosis

As mentioned in Introduction, in this research, images of three types of urinary bladder cancer were used, together with images that represent non-cancer mucosa. The data set consisted of 900 images of non-cancer mucosa, 600 images of high-grade carcinoma, 680 images of low-grade carcinoma and 345 images that represent CIS. All images used in this research were collected and classified by specialist urologist in Clinical Hospital Centre in Rijeka. From a total number of 2525 images, 2020 were used for VGG-16 training, while the rest were used for VGG-16 classification performance evaluation. An example for each class represented in the data set is shown in Figure 2.

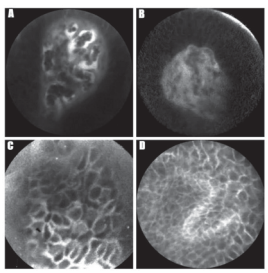

Figure 2: Overview of image data set samples (A: high-grade carcinoma; B : low-grade carcinoma; C: CIS; D: non-cancer mucosa)

VGG-16 ARCHITECTURE

VGG-16 represents one of standard CNN architectures that is used for image classification. It consists of an input layer, 10 convolutional layers (C), 5 pooling layers (P), 3

Table 2: Overview of grid-search procedure used in this research

	Solver	Number of Epochs	Batch size
1	Adam (35)	1	4
2	SGD (36)	2	8
3	RMS-prop (37)	3	16
4	AdaGrad (38)	4	32
5	AdaMax (39)	5	-
6	AdaDelta (40)	6	-
7	Nadam (41)	7	-
8	-	8	-
9	-	9	-
10	-	10	-

fully connected layers (FC) and one output layer (29), as presented in Table 1.

This CNN architecture was introduced in 2014 as a part of ImageNet challenge and it represents an improvement to AlexNet architecture introduced a year earlier (30). AlexNet architecture started a "go deeper" trend in image classification and VGG-16 follows that trend with a difference of using smaller kernels in convolutional layers (31).

RESEARCH METHODOLOGY

In order to determine optimal VGG-16 configuration for bladder cancer diagnosis, multiple variations were trained and tested. VGG-16 models were trained using different solvers for different number of epochs. Furthermore, different batch sizes were used. Solvers represent algorithms that are designed in order to change attributes of neural networks such as weights and learning rates (32). These algorithms were used to reduce the ANN loss, and at the same time, to increase classification performances. Number of epochs represent a number of times in which the total training data set will be propagated through the CNN. Batch size represents the number of images that was propagated through VGG-16 before updating internal model parameters. It is expected that larger batch size will better estimate gradient and therefore it is expected to have better classification performances if lager batches are used (33). Utilization of lager batches requires more GPU memory; therefore, such an approach was omitted (34). Procedure of ANN parameter variation can also be called a "grid-search". Variations of parameters used in this research are presented in Table 2.

In order to evaluate classification performances of each VGG-16 variation, a certain measure must be introduced. In the case of this research, AUC_{micro} is used. AUC_{micro} represents a variation of classical AUC measure adapted to multi-class classification. This measure is based on confusion matrix from which a single scalar value is derived. An example of four-class confusion matrix is given in Figure 3. AUC_{micro} is a value between 0 and 1 where:
1 represents a prefect classification,
0 represents a perfect negative classification and
0.5 represents a random classification.

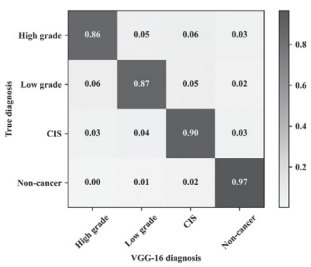

Figure 3: An example of four-class confusion matrix

For the case of four-class classification, confusion matrix C can be written as:

$$C = \begin{bmatrix} C_{11} & C_{21} & C_{31} & C_{41} \\ C_{12} & C_{22} & C_{32} & C_{42} \\ C_{13} & C_{23} & C_{33} & C_{43} \\ C_{14} & C_{24} & C_{34} & C_{44} \end{bmatrix}, \quad (1)$$

where elements on the main diagonal represent ration of correct classification in each class and other elements represent the ration of incorrect classifications in all other classes (42). In order to obtain AUC value, ROC curve must be constructed. ROC curve was constructed by using false positive rate (FPT) and true positive rate (TPR). For the case of AUC_{micro}, TPR can be calculated as:

$$TPR_{micro} = \frac{tr(C)}{G(M)}, \quad (2)$$

where tr(C) represents the trace of the confusion matrix C, calculated as:

$$tr(C) = \sum_{m=1}^{M} C_{mm} \quad (3)$$

and G(C) represents the sum of all elements of the confusion matrix defined as:

$$G(C) = \sum_{m=1}^{M} \sum_{n=1}^{N} C_{mn} \quad (4)$$

On the other hand, for the case of AUC_{micro}, FPR can be calculated as:

$$FPR = \frac{G(C) - tr(C)}{G(C)}. \quad (5)$$

Described measures were used for construction of the ROC curve and determination of AUC_{micro}. AUC_{micro} was, in this case, used as a scalar measure for VGG-16 classification performance evaluation. Using this measures, VGG-16 model that achieves the best classification accuracy was determined.

RESULTS

In the following section, results achieved by using above described grid-search procedure are presented. 3-D plots showing AUC_{micro} value in dependence of number of iteration and batch size are shown for each solver used. When Adam solver is used, it can be noticed that AUC_{micro} values higher than 0.8 are achieved only if VGG-16 was trained with larger batches for more epochs. It can be noticed that maximal AUC_{micro} value of 0.95 was achieved when VGG-16 is trained with batch size of 32 for 10 epochs, as shown in Figure 4.

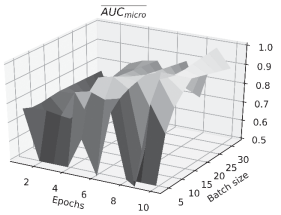

Figure 4: AUC_{micro} *in dependency of number of iteration and batch size for Adam solver*

If SGD solver is used, it can be noticed that AUC_{micro} values higher of 0.8 were achieved regardless of batch size and number of epochs, as shown in Figure 5. Similar to case when VGG-16 is trained by using Adam solver, in this case higher AUC_{micro} values were achieved if higher number of epochs and larger batches were used.

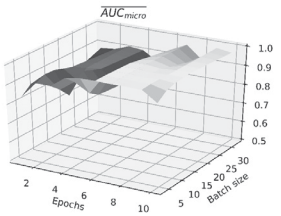

Figure 5: AUC_{micro} *in dependency of number of iteration and batch size for SGD solver*

When RMS-prop solver is used, significantly lower AUC_{micro} values were achieved. Such a characteristic is particularly visible when smaller batches were used and when VGG-16 was trained for lower number of epochs. In this case, AUC_{micro} value does not exceed 0.85, as presented in Figure 6.

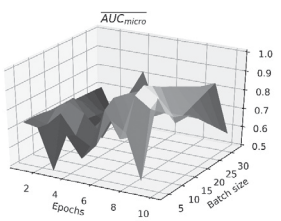

Figure 6: AUC_{micro} *in dependency of number of iteration and batch size for RMS-prop solver*

When AdaGrad solver was used, AUC_{micro} values higher than 0.8 were achieved. This property is visible regardless of batch size and number of epochs. Such a characteristic is presented in Figure 7. Maximal value of 0.98 was achieved if VGG-16 was trained for higher number of epochs by using lager batches.

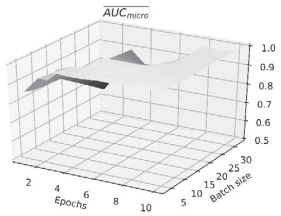

Figure 7: AUC_{micro} *in dependency of number of iteration and batch size for Adagrad solver*

Similarly, in the case when AdaMax solver was used, the vast majority of different variations of VGG-16 were achieving AUC_{micro} values higher than 0.9. In this case, difference is in the cases that were trained for lower number of epochs. These variations achieve lower classification performances, as presented in Figure 8.

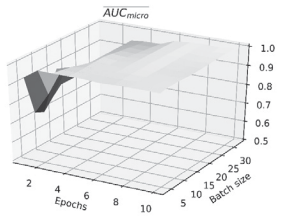

Figure 8: AUC_{micro} *in dependency of number of iteration and batch size for AdaMax solver*

When AdaDelta solver was used, the highest AUC_{micro} values were achieved if VGG-16 is trained for larger number of iterations. In this case, it is interesting to notice that higher AUC_{micro} values were achieved if VGG-16 was trained by using smaller batches of data. Such a property is presented in Figure 9.

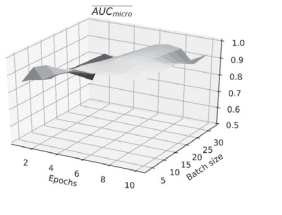

Figure 9: AUC_{micro} *in dependency of number of iteration and batch size for AdaDelta solver*

As the last case, VGG-16 trained with Nadam solver is observed. It can be noticed that in this case, AUC_{micro} does not exceed 0.8, as presented in Figure 10. VGG-16 CNN shows a poor performance across all hyperparameter combinations when trained by using Nadam solver.

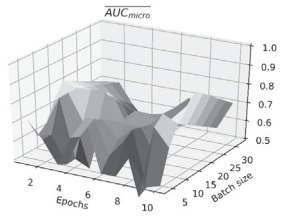

Figure 10: AUC_{micro} *in dependency of number of iteration and batch size for Nadam solver*

DISCUSSION

When all AUC_{micro} values achieved with different solvers are compared, it can be noticed that the highest classification performances are achieved if AdaGrad and AdaMax solvers were used for VGG-16 training. High performances were also achieved if Adam, SGD and AdaDelta solvers were used. On the other hand, poor classification performances were achieved with RMS-prop and Nadam solvers, as presented in Figure 11.

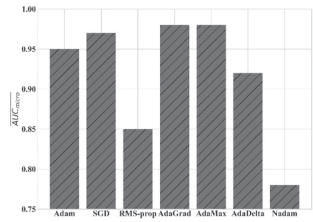

Figure 11: Comparison of achieved AUC_{micro} *values for different solvers*

When results presented in this article are compared to results from the literature overview, it can be noticed that similar performances are achieved although four-class classification was performed. VGG-16 trained by using AdaGrad or AdaMax solver with up to 0.98 can be compared with results presented in (26 – 28).

From presented results, it can be noticed that VGG-16 architecture achieves high perfor-

mance. Such high performance is achieved in both cancer diagnosis and cancer grade recognition. Presented results are pointing towards the possibility of a clinical application of an AI-based algorithm, not only in the context of the bladder cancer diagnosis but also in the context of grade recognition.

CONCLUSIONS

In this paper, the diagnostic approach for urinary bladder cancer using VGG-16 architecture is presented. From presented results it can be noticed that high classification performances can be achieved if specific variation of VGG-16 architecture is used. The best classification performances are achieved if VGG-16 is trained by using AdaGrad or AdaMax solver for 8-10 epochs. Also, it can be noticed that these performances were achieved when VGG-16 architecture is trained by using larger data batches. These results have enabled to increase accuracy of urinary bladder cancer type recognition. Consequently, obtained results are showing promising possibility for achieving higher accuracy of CIS diagnosis.

AKNOWLEDGEMENTS

This research has been (partly) supported by the CEEPUS network CIII-HR-0108, European Regional Development Fund under the grant KK.01.1.1.01.0009 (DATACROSS), project CEKOM under the grant KK.01.2.2.03.0004, CEI project "COVIDAi" (305.6019-20) and University of Rijeka scientific grant uniri-tehnic-18-275-1447

BIBLIOGRAPHY

1. Hrvatski zavod za javno zdravstvo [Internet]. Cancer incidence in Croatia 2015 [cited 2021 Jan 25]. Available from: https://www.hzjz.hr/en/statistical-data/cancer-incidence-in-croatia-2015/
2. Cancer Genome Atlas Research Network. Comprehensive molecular characterization of urothelial bladder carcinoma. Nature. 2014 Mar 20;507(7492):315.
3. Takahashi K, Kimura G, Endo Y, Akatsuka J, Hayashi T, Toyama Y, et al. Urothelial carcinoma of the bladder, lipid cell variant: A case report and literature review. J. Nippon Med. Sch.. 2019:JNMS-2019_86.
4. Dotson A, May A, Davaro F, Raza SJ, Siddiqui S, Hamilton Z. Squamous cell carcinoma of the bladder: poor response to neoadjuvant chemotherapy. Int. J. Clin. Oncol.. 2019 Jun;24(6):706-11.
5. Celis JE, Wolf H, Østergaard M. Bladder squamous cell carcinoma biomarkers derived from proteomics. Electrophoresis2000 Jun 1;21(11):2115-21.
6. Dadhania V, Czerniak B, Guo CC. Adenocarcinoma of the urinary bladder. Am. J. Clin. Exp. Urol.. 2015;3(2):51.
7. Sharma A, Fröhlich H, Zhang R, Ebert AK, Rösch W, Reis H, et al. Classic bladder exstrophy and adenocarcinoma of the bladder: Methylome analysis provide no evidence for underlying disease-mechanisms of this association. Cancer Genetics. 2019 Jun 1;235:18-20.
8. Ismaili N. A rare bladder cancer-small cell carcinoma: review and update. Orphanet J. Rare Dis. 2011 Dec 1;6(1):75.
9. Gil RT, Esteves G. Small cell carcinoma of the urinary bladder: a rare and aggressive tumor. Acta Radiológica. 2019 Jan;31(1):23-6.
10. Mitra S, Kaur G, Kakkar N, Singh P, Dey P. Sarcoma in urine cytology; an extremely rare entity: A report of two cases. J. Cytol.. 2017 Jul;34(3):171.
11. Daga G, Kerkar P. Sarcomatoid carcinoma of urinary bladder: a case report. Indian J.l Sur. Onc.. 2018 Dec 1;9(4):644-6.
12. Tanagho EA, McAninch JW. Smith s general urology. 17th ed. Lange Medical Books/McGraw-Hill; 2004.
13. Zlatev DV, Altobelli E, Liao JC. Advances in imaging technologies in the evaluation of high-grade bladder cancer. Urologic Clinics. 2015 May 1;42(2):147-57.
14. Duty BD, Conlin MJ. Principles of urologic endoscopy. Campbell-Walsh Urology. 11th ed. Philadelphia, PA: Elsevier. 2016:136-52.
15. Lerner SP, Liu H, Wu MF, Thomas YK, Witjes JA. Fluorescence and white light cystoscopy for detection of carcinoma in situ of the urinary bladder. In Urologic Oncology: Seminars and Original Investigations 2012 May 1 (Vol. 30, No. 3, pp. 285-289). Elsevier.
16. Shah M, Naik N, Somani BK, Hameed BZ. Artificial intelligence (AI) in urology-Current use and future directions: An iTRUE study. Turk. J. Uro. 2020 Nov;46(Suppl 1):S27.
17. Lorencin I, Anđelić N, Mrzljak V, Car Z. Multilayer perceptron approach to condition-based maintenance of marine CODLAG propulsion system components. Pomorstvo. 2019 Dec 19;33(2):181-90.
18. Baressi Šegota S, Lorencin I, Musulin J, Štifanić D, Car Z. Frigate Speed Estimation Using CODLAG Propulsion System Parameters and Multilayer Perceptron. Naše More. 2020 May 18;67(2):117-25.
19. Lorencin I, Anđelić N, Mrzljak V, Car Z. Genetic algorithm approach to design of multi-layer perceptron for combined cycle power plant electrical power output estimation. Energies. 2019 Jan;12(22):4352.
20. Lorencin I, Anđelić N, Mrzljak V, Car Z. Marine objects recognition using convolutional neural networks. Naše More. 2019 Sep 26;66(3):112-9.
21. Musulin J, Štifanić D, Lorencin I, Baressi Šegota S, Anđelić N, Borović E, et al. Comparison of Three Artificial Intelligence Algorithms for Sepsis Prediction. World of Health, 3, 13. 2020;19.
22. Lorencin I, Anđelić N, Baressi Šegota S, Štifanić D, Musulin J, Mrzljak V, et al. Dataset Size-based Approach in Design of Artificial Neural Network for Breast Cancer Diagnosis. World of Health, 3, 13. 2020;19.
23. Car Z, Baressi Šegota S, Anđelić N, Lorencin I, Mrzljak V. Modeling the Spread of COVID-19 Infection Using a Multilayer Perceptron.

Comput. Math. Methods Med .2020 May 29;2020.
24. Anđelić N, Baressi Šegota S, Lorencin I, Mrzljak V, Car Z. Estimation of COVID-19 epidemic curves using genetic programming algorithm. Health Inform. J.2021 Jan;27(1):1460458220976728.
25. Ikeda A, Nosato H, Kochi Y, Kojima T, Kawai K, Sakanashi H, et al. Support system of cystoscopic diagnosis for bladder cancer based on artificial intelligence. J. Endourology. 2020 Mar 1;34(3):352-8.
26. Bogović K, Lorencin I, Anđelić N, Blažević S, Smolčić K, Španjol J, et al. Artificial intelligence-based method for urinary bladder cancer diagnostic. In International Conference on Innovative Technologies, IN-TECH 2018 2018 Jan 1.
27. Eminaga O., Semjonow A., Breil B. Diagnostic classification of cystoscopic images using deep convolutional neural networks. JCO. 2018 Oct;2:1-8.
28. Lorencin I, Anđelić N, Španjol J, Car Z. Using multi-layer perceptron with Laplacian edge detector for bladder cancer diagnosis. Artif. Intell. in Med.2020 Jan 1;102:101746.
29. Lorencin I, Baressi Šegota S, Anđelić N, Blagojević A, Šušteršić T, Protić A, et al. Automatic Evaluation of the Lung Condition of COVID-19 Patients Using X-ray Images and Convolutional Neural Networks. J. . Pers. Med.2021 Jan;11(1):28.
30. Guan Q, Wang Y, Ping B, Li D, Du J, Qin Y, et al. Deep convolutional neural network VGG-16 model for differential diagnosing of papillary thyroid carcinomas in cytological images: a pilot study. J.Cancer. 2019;10(20):4876.
31. Geng L, Zhang S, Tong J, Xiao Z. Lung segmentation method with dilated convolution based on VGG-16 network. Comput. Assist. Surg2019 Oct 7;24(sup2):27-33.
32. Baressi Šegota S, Anđelić N, Kudláček J, Čep R. Artificial neural network for predicting values of residuary resistance per unit weight of displacement. Pomorski zbornik. 2019 Dec 31;57(1):9-22.
33. Radiuk PM. Impact of training set batch size on the performance of convolutional neural networks for diverse datasets. Information Technology and Management Science. 2017 Dec 20;20(1):20-4.
34. You Y, Gitman I, Ginsburg B. Scaling sgd batch size to 32k for imagenet training. arXiv preprint arXiv:1708.03888. 2017 Sep 16;6.
35. Baressi Šegota S, Lorencin I, Anđelić N, Mrzljak V, Car Z. Improvement of Marine Steam Turbine Conventional Exergy Analysis by Neural Network Application. J. Mar. Sci. Eng. 2020 Nov;8(11):884.
36. Yang J, Yang G. Modified convolutional neural network based on dropout and the stochastic gradient descent optimizer. Algorithms. 2018 Mar;11(3):28.
37. Bengio Y, CA M. Rmsprop and equilibrated adaptive learning rates for nonconvex optimization. corr abs/1502.04390. 2015.
38. Ward R, Wu X, Bottou L. AdaGrad stepsizes: Sharp convergence over nonconvex landscapes. InInternational Conference on Machine Learning 2019 May 24 (pp. 6677-6686).
39. Zeng X, Zhang Z, Wang D. AdaMax Online Training for Speech Recognition. 2016. 2016.
40. Zeiler MD. Adadelta: an adaptive learning rate method. arXiv preprint arXiv:1212.5701. 2012 Dec 22.
41. Wang J, Cao Z. Chinese text sentiment analysis using LSTM network based on L2 and Nadam. In2017 IEEE 17th International Conference on Communication Technology (ICCT) 2017 Oct 27 (pp. 1891-1895). IEEE.
42. Lorencin I, Anđelić N, Šegota SB, Musulin J, Štifanić D, et al. Edge Detector-Based Hybrid Artificial Neural Network Models for Urinary Bladder Cancer Diagnosis. In Enabling AI Applications in Data Science (pp. 225-245). Springer, Cham.